Journal of Applied Polymer Science

Preparation, characterization, electrical and antibacterial properties of sericin/poly(vinyl alcohol)/poly(vinyl pyrrolidone) composites

M. T. Ramesan,[1] V. K. Athira,[1] P. Jayakrishnan,[1] C. Gopinathan[2]

[1]Department of Chemistry, University of Calicut, Calicut University Post Office, Kerala 673 635, India

[2]Department of Biotechnology, University of Calicut, Calicut University Post Office, Kerala 673 635, India

Correspondence to: M. T. Ramesan (E-mail: mtramesan@uoc.ac.in)

ABSTRACT: In this study, we focused on the fabrication of poly(vinyl alcohol) (PVA)/poly(vinyl pyrrolidone) (PVP)/sericin composites via a simple solution-blending method. The composites were characterized by Fourier transform infrared (FTIR) spectroscopy, UV spectroscopy, X-ray diffraction (XRD), scanning electron microscopy (SEM), differential scanning calorimetry, thermogravimetric analysis (TGA), and measurements of the conductivity, tensile strength, and antibacterial activity against *Staphylococcus aureus*. The results of FTIR and UV spectroscopy implied the occurrence of hydrogen bonding between sericin and the PVA/PVP blend. The structure and morphology, studied by XRD and SEM, revealed that the sericin particles were well dispersed and arranged in an orderly fashion in the blend. The glass-transition temperature (T_g) of the composite was higher than that of the pure blend, and the T_g value shifted toward higher temperatures when the volume fraction of sericin increased. TGA indicated that sericin retarded the thermal degradation; this depended on the filler concentration. The mechanical and electrical properties, such as the tensile strength, alternating-current electrical conductivity, dielectric constant, and dielectric loss of the composites, were higher than those of the pure blend, and these properties were enhanced when the concentration of sericin was increased up to 10 wt % filler content, whereas the elongation at break of the composite decreased with the addition of sericin particles. The antibacterial properties of the composite showed that sericin had a significant inhibitory effect against *S. aureus*. © 2016 Wiley Periodicals, Inc. J. Appl. Polym. Sci. **2016**, *133*, 43535.

KEYWORDS: blends; composites; differential scanning calorimetry (DSC); mechanical properties; thermal properties

Received 11 November 2015; accepted 12 February 2016

DOI: 10.1002/app.43535

INTRODUCTION

Polymer blends draw great attention because of their large number of applications; these applications include those in electronics, photonics, biotechnology, and electrochemical sensors. Compared to pristine polymers, polymer blends possess many desirable properties, including enhanced gas-barrier properties, corrosion resistance, ionic conductivity, thermal stability, and mechanical strength.[1–3] These mechanical properties depend on the degree of compatibility of blend, and a high degree of compatibility indicates higher interaction between the polymeric phases of the polymer blend.[4,5] Therefore, different functional groups containing polymers allow the resulting blends to be compatible with a significant mechanical performance.

In this world, the production and utilization of petroleum-based polymer has increased considerably, but these polymers do not readily enter the degradation cycles of the biosphere. To support their continued sustainable development in the world, this problem must be addressed. There is increasing interest in replacing synthetic polymers with biodegradable materials. Hence, the enhancement of biodegradability is an important issue in the industrial application of biodegradable polymers. In this context, the blending of poly(vinyl alcohol) (PVA) and poly(vinyl pyrrolidone) (PVP) leads to a water-soluble and biodegradable polymer with improved mechanical properties.[6–8]

Sericin is a natural, macromolecular water-soluble protein derived from silk cocoons. The silk fibers are composed of a protein fibroin with sericin surrounding it, and the removal of sericin from silk fiber is accomplished by a process called degumming.[9] Most of the sericin must be removed during raw silk processing in the reeling mill and in other stages of silk production. At present, silk sericin is mostly discarded as wastewater, and this causes environmental pollution.[10] The recycling of sericin protein from waste sericin water could lead to significant economic and social benefits. Sericin is composed of several amino acids with polar groups, such as hydroxyl, carbonyl, and amine groups.[11] Recently, the outstanding properties of

sericin have attracted the attention of researchers, and it is widely used in biomedical applications because of its biocompatibility and biodegradability.[12–15] Kaitsuka and Goto[16] reported the fabrication of an optically active and electrically conductive polyaniline composite with different contents of sericin particles. However, sericin has some drawbacks, including poor mechanical properties and poor thermal stability. Sericin particles contain several polar groups, such as amide, carboxyl, and carbonyl groups, which are miscible with the hydroxyl group of PVA or with the carbonyl group of PVP, and therefore matrix, the study of their structure, morphology, thermal stability, and electrical properties is important.

Environmental conservation is a prime concern, and several studies[17–19] have been carried to convert waste materials into useful ones. These studies are very attractive from both ecological and economic points of view. Efforts to find ways to use to waste materials have resulted in mostly valuable products. In this respect, waste sericin seems to be an interesting candidate because of the large number of functional groups on the surface of sericin particles. The utilization of waste sericin from the silk industry has not yet been properly explored for the fabrication of polymer composites. Hence, the novelty of this study will be appealing to both the common and scientific community from mainly economic and ecological points of view. In this study, we focused on the use of a simple, inexpensive, and environmentally friendly solution-casting method to fabricate sericin/PVA/PVP blends. The fabricated polymer blends composites were structurally characterized by Fourier transform infrared (FTIR) spectroscopy, UV spectroscopy, X-ray diffraction (XRD), scanning electron microscopy (SEM), differential scanning calorimetry (DSC), and thermogravimetric analysis (TGA). In this study, we also focused on the influence of sericin on the mechanical, electrical, and antibacterial properties of these multifunctional composites.

EXPERIMENTAL

Materials and Methods

PVA, with an average molecular weight of 72,000, and PVP, with a molecular weight mass of 40,000, were purchased from Himedia (Mumbai, India). Both polymers were used without further purification. *Bombyx mori* (*B. mori*) cocoons were kindly supplied by Central Sericulture Research and Training Institute (Mysore, India). A *Staphylococcus aureus* pure culture was procured from Calicut Medical College (Kerala, India) and was maintained at 4 °C on nutrient agar slants.

Preparation of Sericin Powder

Sericin was extracted from the waste cocoons of the *B. mori* silkworm with a high-temperature and high-pressure technique.[20] The cocoons were cut into small pieces, and sericin was then extracted with hot water under pressure at 120 °C for 60 min with an autoclave. After cooling, the solution was filtered with filter paper to remove the fibroin fibers. The remaining solution was then deep-frozen at −20 °C to enhance precipitation. The frozen solution was defrosted and filtered *in vacuo*.

Preparation of the PVA/PVP/Sericin Composites

PVA and PVP solutions were prepared separately by the dissolution of required amounts of PVA and PVP in double-distilled water at 70 °C. The two solutions were then mixed (at a 50:50 PVA/PVP) and stirred until the solution become homogeneous. A required quantity of sericin (0, 3, 5, 7, 10, and 15 wt %) was added to the previous homogeneous polymer blend solution. The mixture was stirred until the solution became homogeneous. Finally, the viscous solution was poured into a Petri dish and dried at 60 °C for 2 days.

Analytical Methods

The ultraviolet–visible (UV–vis) absorption spectra of the blend and different loadings of sericin particles containing the blend composite in water were recorded on a Hitachi U-3000 spectrophotometer. The FTIR spectra of the blend and blend composite were recorded on a Jasco (model 4100) FTIR spectrophotometer in the wave-number region of 400–4000 cm^{-1} at a resolution of 2 cm^{-1} and a scan frequency of 16 times. XRD patterns of the powdered sample were recorded on a Bruker AXS D X-ray diffractometer with Cu Kα radiation ($\lambda = 1.5406$ Å) with an accelerating voltage of 30 kV. The diffractograms were recorded in terms of 2θ in the range 10–80°. The surface structure of the film sample was investigated with field emission scanning electron microscopy (FESEM; Hitachi, SU 6600 FESEM instrument) after gold coating. DSC studies were carried out on a V2 6D TA instrument (model DSC 2010) at a heating rate of 10 °C/min. Initial scans were taken from 50 to 100 °C to remove the thermal history effects and then cooled to room temperature. The scans were recorded at a heating rate of 10 °C/min in the temperature range from 30 to 350 °C. The thermal stability of the resulting composites were investigated by a PerkinElmer thermogravimetric analyzer with pure nitrogen at a flow rate of 20 mL/min and a heating rate of 10 °C/min. We measured the electrical conductivity of the polymer film by cutting the samples into a circular shape. The alternating-current (ac) resistivity of the samples was measured with a Hewlett–Packard LCR meter (LCR meter is a type of electronic test equipment used to measure the inductance (L), capacitance (C), and resistance (R) of an electronic component) fully automatic system in the frequency range 10^2-10^6 Hz at room temperature. The dielectric constant, or relative permittivity (ε_r), was calculated with the following formula:

$$\varepsilon_r = \frac{Cd}{\varepsilon_0 A} \quad (1)$$

where C is the capacitance, d is the thickness of the sample, A is the area of the cross section of the sample, and ε_0 is the permittivity of free space, a dimensionless quantity. From these measurements, the ε_r and dielectric loss ($\tan\delta$) values of the composites were determined. The tensile strength of the blend and its composites were carried out according to BS 6746 with an Instron 4301 universal testing machine (Lancashire, United Kingdom). The test was carried out with dumbbell-shaped tensile specimens at a crosshead speed of 500 mm/min at room temperature. Five specimens of each sample were subjected to tensile testing, and their average values are reported.

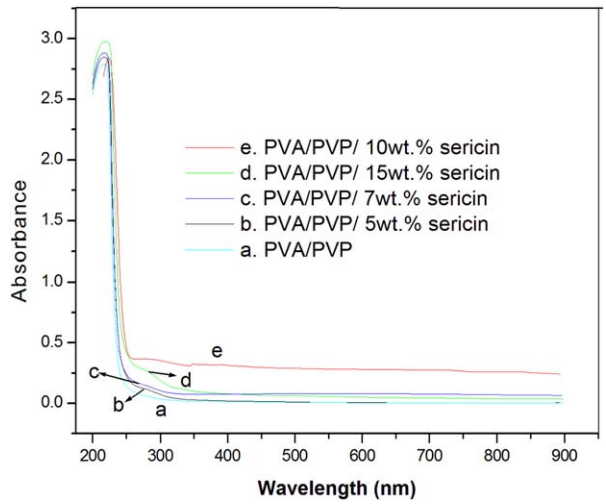

Figure 1. UV–vis spectra of the PVA/PVP blends with various concentrations of sericin particles. [Color figure can be viewed in the online issue, which is available at wileyonlinelibrary.com.]

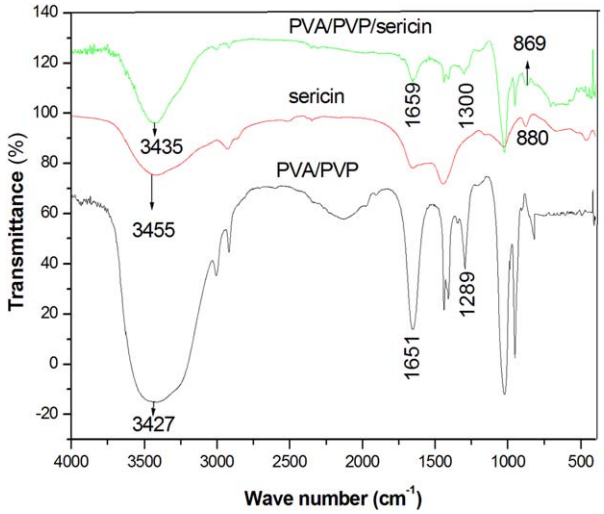

Figure 2. FTIR spectra of the sericin, PVA/PVP, and sericin-incorporated PVA/PVP blend. [Color figure can be viewed in the online issue, which is available at wileyonlinelibrary.com.]

Antibacterial Activity against *S. aureus*. We studied the antibacterial activity of the blend and its composites by performing an agar well diffusion assay. For this, 100 mL of nutrient agar medium was made and sterilized at 50 psi for 15 min. The molten medium was poured into a sterile Petri dish with an airflow cabinet. After solidification, 0.1 mL of a bacterial culture of *S. aureus* was inoculated into a Petri dish containing the agar medium, and it was spread smoothly on the surface with a sterile glass spreader. With a sterile test tube, a well was cut into the center of the agar medium. A volume of 0.5 mL of blend and its composite was added to the well with a sterile pipette, the Petri dishes were incubated at 37 °C for 24 h, and the zone of inhibition was visualized. These experiments were done in triplicate.

RESULTS AND DISCUSSION

Optical Properties

The variations of the optical absorbance of the PVA/PVP blend with various concentrations of sericin particles over a wavelength of 200–900 nm were recorded at room temperature and are illustrated in Figure 1. The π–π^* transition of the PVA/PVP blend showed a sharp absorption peak at 216 nm, whereas the samples with 5, 7, 10, and 15 wt % sericin-incorporated blend exhibited UV absorption peaks at 217, 218, 224, and 221 nm, respectively. The spectra indicated that the absorbance of the composite was higher than that of the pure blend, and the absorbance of the composite increased with increasing concentration of sericin particles up to 10 wt %. Thereafter, the absorbance decreased with the further addition of sericin in the entire region from 200 to 900 nm. The high absorption efficiency of the composite (10 wt %) was due to the uniform distribution of sericin particles in the polymer matrix. Moreover, the intermolecular interaction (H bonding) between the amino group of sericin particles and the hydroxyl group of the blend segments led to the absorbance of more light.[21] At higher concentrations of sericin, the dispersability of particles decreased because of the aggregation of sericin, which resisted the absorption of incident light.

FTIR Characterization

Figure 2 shows the FTIR spectra of the sericin, PVA/PVP blend, and PVA/PVP/sericin in the range 4000–400 cm^{-1}. The major absorption band positions and their assignments for these samples are listed in Table I. A strong band in wave-number range 3200–3500 cm^{-1} was assigned to the OH stretching vibrations of the PVA/PVP blend. Another sharp peak at 1651 cm^{-1} was attributed to the stretching vibrations of C=C and the methyl

Table I. Position of the Absorption Bands and the Assignments for the Sericin, PVA/PVP Blend, and Blend Composites

Material	Wave number (cm^{-1})	Assignment
Sericin	3455	NH stretching
	1662	C=O stretching
	1457	Amide I bending
	880	Amide II bending
PVA/PVP	3427	OH stretching
	1651	C=C stretching
	1289	CH_2 bending
	1027	C=O stretching
	945	CO symmetrical stretching
PVA/PVP/sericin	3435	OH and NH stretching
	1659	C=O stretching
	1201	CH_2 bending
	1300	Bending OH or amide
	1023	C=O stretching, CH and OH bending
	952	CO symmetrical stretching
	869	Amide bending

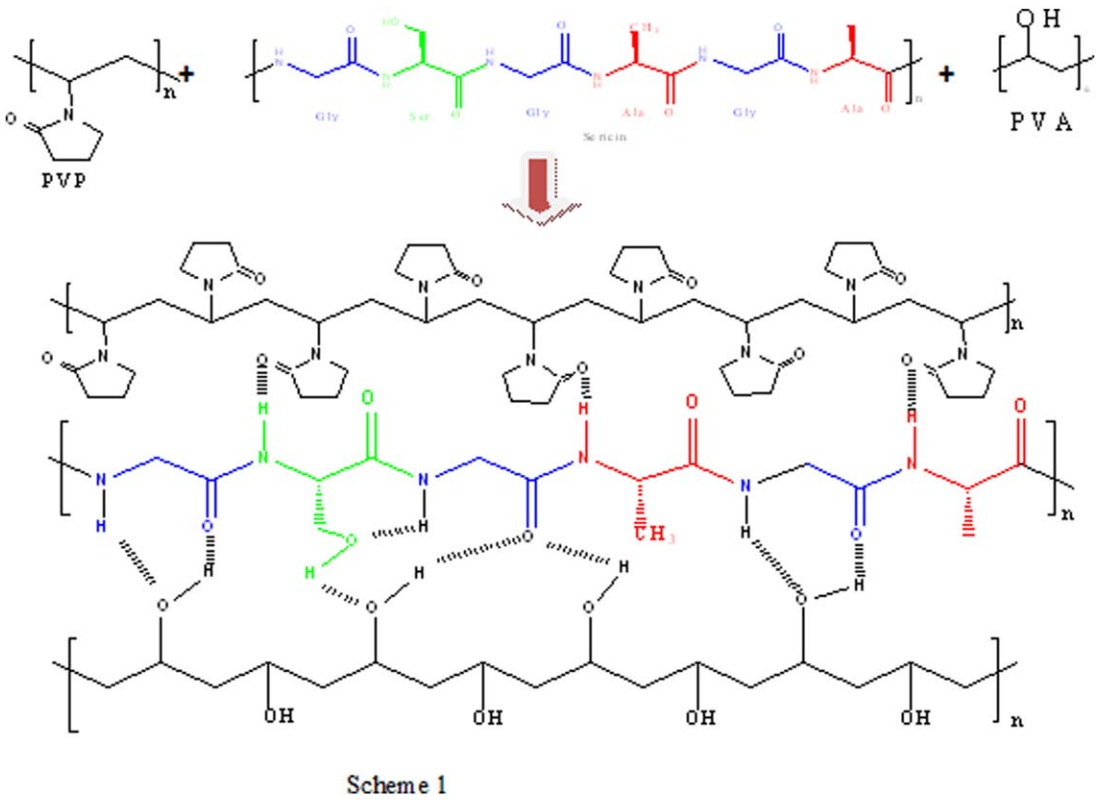

Scheme 1. Mechanism of interaction between sericin and the PVA/PVP blend. [Color figure can be viewed in the online issue, which is available at wileyonlinelibrary.com.]

groups of the PVA/PVP blend.[22,23] The characteristic stretching of PVP was observed at 1289 cm^{-1}. The FTIR spectrum of sericin powder exhibited a broad band at 3455 cm^{-1}; this was related to the NH group of sericin. Furthermore, the characteristic bands at 1659 and 1439 cm^{-1} were attributed to the C═O group of sericin, and a shoulder appeared at 869 cm^{-1}, which corresponded to the secondary amine group of the filler particles.[24] However, the spectra of the PVA/PVP/sericin composites showed almost all of the characteristic peaks of the blend and the sericin particles. A comparison of the IR spectra of the blend and the sericin-containing polymer blend revealed a new band positioned at 1300 cm^{-1}. This was attributed to the intermolecular interaction between the surface of the electronegative particles in sericin and the polar groups in the macromolecules. Also, the broad absorption of the composites shifted toward higher wave numbers from 3427 to 3435 cm^{-1}, and this was also due to the hydrogen-bonding interactions between sericin and the polymer.[25] The interaction of the amino groups of sericin with the hydroxyl or carbonyl groups of PVA and PVP is given in Scheme 1.

XRD

XRD was used to analyze the structure and composition of the polymer composite. The XRD curves of sericin, PVP/PVP, and different concentrations of sericin-particle-incorporated PVP/PVP blends are presented in Figure 3. The sericin particles showed a broad characteristics amorphous peak at a 2θ of 20.1°. The XRD curve of PVP/PVP showed a broad diffraction peak at a 2θ of 20.9°; this indicated the amorphous regions of PVA and PVP. The blend also showed a couple of bands located at 2θs of 29.4 and 47.8°; this clearly indicated its semicrystalline nature. This was due to the strong hydrogen-bonding interactions between the OH groups of PVA and the carbonyl groups in PVP; this led to an orientation of the macromolecular chain of the blend.[26] The XRD pattern of 10 wt % sericin/PVP/PVP composite showed a sharp diffraction peak at a 2θ of 27.3°, and

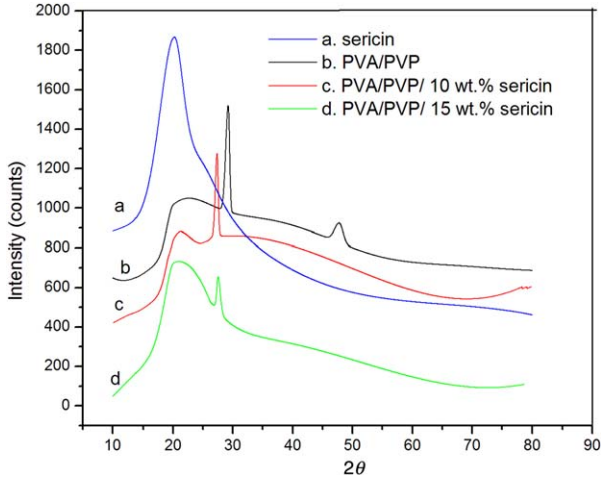

Figure 3. XRD patterns of the sericin, PVA/PVP, and sericin-containing PVA/PVP blend. [Color figure can be viewed in the online issue, which is available at wileyonlinelibrary.com.]

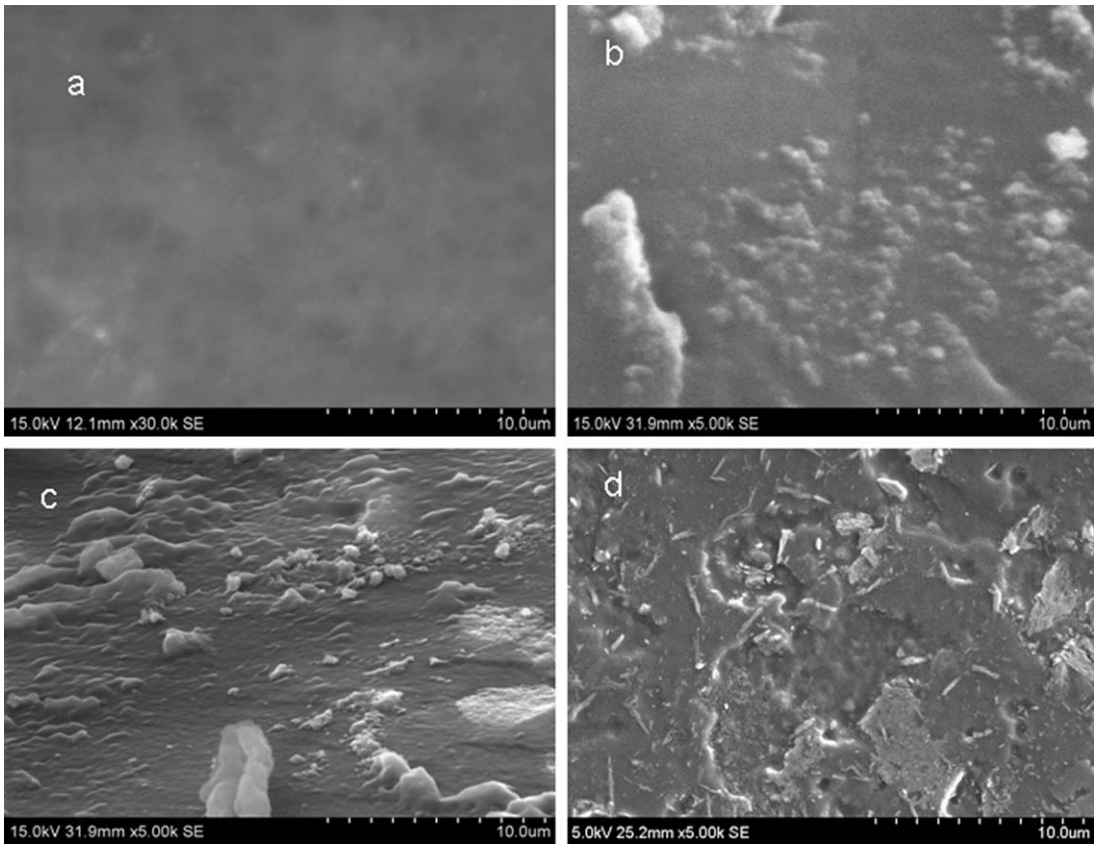

Figure 4. SEM images of the (a) PVA/PVP blend, and blends with (b) 5, (c) 10, and (d) 15 wt % sericin.

we also observed that the peak at a 2θ of 47.8° was absent. However, when the concentration of sericin particles was 15 wt %, the intensity of the crystalline peak at a 2θ of 27.3° decreased, and the amorphous region become more prominent at a 2θ of 20.6°. Therefore, we inferred that the sericin particles were strongly trapped in the macromolecular chain of the blends because of the strong polar–polar interactions between the sericin and blend segments.

FESEM

Figure 4 shows the FESEM morphology of PVA/PVP and its blends with different weight percentages of sericin particles. As shown in the SEM images [Figure 4(a)], the pristine blend had a smooth surface; this indicated that the both the PVA and PVP segments were compatible mixtures because of the strong intermolecular interactions between them. The SEM images of a lower concentration of the hybrid materials [Figure 4(b,c)] showed a uniform morphology, and the sericin particles were well dispersed into the macromolecular chain of the blend. This was due to the interfacial interaction between the polar segments of sericin particles and the polar unit of the blend. However, in the case of higher concentrations of sericin particles [Figure 4(d)], the morphology of the hybrid totally changed, the sample expanded slightly, and the particles formed clusters. It was noteworthy that a lower concentration of sericin particles was more efficiently inserted into the blend than a higher concentration (15 wt %).

DSC

Figure 5 shows the DSC analysis of the PVA/PVP and sericin-particle-incorporated PVA/PVP blend in the temperature range from 0 to 350 °C. For the pure blend [Figure 5(a)], the DSC curve showed a major endothermic peak centered at about 114 °C; this was assigned to the glass-transition temperature (T_g) of the polymer blend. The endothermic peaks, which

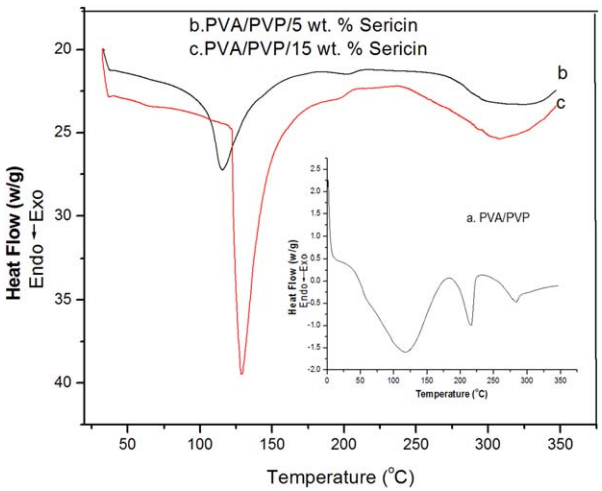

Figure 5. DSC plots of the PVA/PVP blends and their composites with different loadings of sericin particles. [Color figure can be viewed in the online issue, which is available at wileyonlinelibrary.com.]

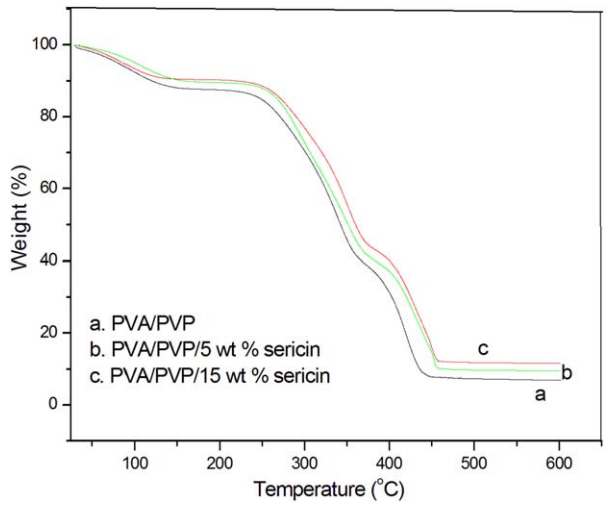

Figure 6. TGA curves of the PVA/PVP blends with different concentrations of sericin. [Color figure can be viewed in the online issue, which is available at wileyonlinelibrary.com.]

appeared at 215 and 283 °C, in the polymer blend were related to the melting temperatures of PVA and PVP, respectively. It is clearly shown in the figure that the samples with 5 and 15 wt % sericin [Figure 5(b,c)] showed T_gs at 116 and 128 °C with melting temperatures around 307 and 310 °C, respectively. The increase in the T_g of composites with increasing concentration of sericin was due to the strong intermolecular interactions (hydrogen bonding) developed between the PVA/PVP blend with the different functional groups containing sericin. Hence, we concluded that the thermal properties, such as T_g, depended on the concentration of sericin particles.

TGA

Figure 6 shows the effect of various contents (weight percentages) of sericin powder on the thermal stability of the PVA/PVP blend examined by TGA, and the DTG curve of the samples are given in Figure 7. All of the compounds underwent three stages of thermal degradation. The first one appeared around 70–140 °C, and this showed about a 10.13% weight loss, which was assigned to the removal of acetic acid and physically adsorbed water molecules. The second major decomposition occurred in the temperature range 220–360 °C. During this stage, the decomposition was a 35% weight loss. This was associated with the melting of the blend segments. The third degradation step started around 370 to 460 °C, with a weight loss of 30%, and this was the consequence of the cyclization and condensation process of the polyaromatic structures.[27] As shown in the figure, it was clear that the blend composite showed a higher thermal stability than the pure blend, and the thermal stability increased with increasing concentration of sericin particles. The increase in the thermal stability was due to the hydrogen-bond interaction between the blend and the different functional-group-containing sericin particles; this impended heat diffusion to the blend matrix. The degradation temperature and the char residue at 500 °C for the PVA/PVP blend and its composite with sericin particle are shown in Table II. The initial degradation temperature ($T_{5\%}$) of the blend was found to 353.33 °C, whereas the blend composite with 10 wt % sericin compound had a $T_{5\%}$ of 373.61 °C. This indicated that the incorporation of sericin particles improved the thermal resistance of the PVA/PVP matrix. It was also evident from Table II that the final char residue of the composite was higher than that of the unfilled blend. The increase in char residue with increasing concentration of sericin particles indicated the improved flame resistance of the polymer composite.[28]

Kinetic Analysis of Thermal Decomposition

TGA data was used to measure the kinetic parameters, such as the apparent activation energy (E), pre-exponential factor, and order of reaction in the thermal decomposition reaction. The observed changes in the mechanisms led to a unique thermal behavior and, hence, a better knowledge of the materials. Several methods have been reported for calculating the kinetic parameters of solid-state reactions. The Coats–Redfern method[29] is one of the best correlation techniques for evaluating the relation between g(α), a thermogravimetric function with $1/T$, according to following (rate of reaction) equation:

$$\ln\left[\frac{g(\alpha)}{T^2}\right]=\ln\left(\frac{AR}{\Phi_E}\right)\left(1-\frac{2RT}{E}\right)-\frac{E}{RT} \quad (2)$$

where g(α) is rate of reaction $\left[g(\alpha)=\int\frac{d\alpha}{dt}\right]$, T is temperature in Kelvin Scale, Φ_E is temperature change $\left[\Phi_E=\frac{dT}{dt}\right]$, α is the degree of conversion and is depend with heating rate

$$\alpha=\frac{Ci-C}{C_i-C_f} \quad (3)$$

where α is the heating rate, E is the apparent activation energy for decomposition, C is the weight of sample at a specific temperature, and C_i and C_f are the weights at the initial and final temperatures, respectively. E is determined from the plot of the variation of $\ln[g(\alpha)/T^2]$ versus $1/T$. The slope of each plot is used to find E. The best linear fit model of the kinetic parameters gives the maximum correlation coefficient (R) from the graph, and that value was found to be very close to 1. The results obtained from the Coats–Redfern method are tabulated

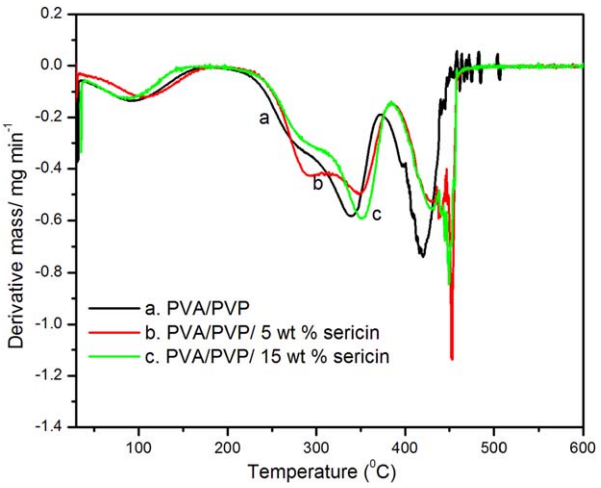

Figure 7. DTG analysis of the PVA/PVP blends with different contents of sericin. [Color figure can be viewed in the online issue, which is available at wileyonlinelibrary.com.]

Table II. Degradation Temperature and *E* Values of the PVA/PVP Blend and Its Composites with Sericin Particles

Sample	$T_{5\%}$ (°C)	Temperature at 15% degradation (°C)	Final residue (%)	*E* (kJ/mol)	*R*
PVA/PVP	353.33	521.57	6.86	51.99	0.99963
PAV/PVP/5 wt % sericin	359.49	545.05	9.54	53.16	0.99995
PAV/PVP/10 wt % sericin	373.61	540.98	11.63	54.31	0.99997

in Table II, and the representative plots of the Coats–Redfern equation for the PVA/PVP blend and its composite with sericin particle are presented in Figure 8. As shown in Table II, it was clear that *E* of blend composite was higher than that of the pure blend, and *E* was found to increase with the increasing concentration of sericin particles. The increased value of *E* confirmed the higher thermal stability of the blend composite compared to that of PVA/PVP, and this was mainly attributed to the enhanced intermolecular interactions between the polar segments of the blend with the polar domain of sericin particles.

Effects of the Loading of Sericin Particles on the Mechanical Properties

The effects of the loading of sericin particles on the tensile strength and elongation at break (EB) of the PVA/PVP blend are given in Figure 9. An increase in the tensile strength was observed with increasing sericin content up to 10 wt %. This indicated a more uniform dispersion of sericin in the blend up to 10 wt % loading; in other words, this loading provided a large interfacial area of contact with the polar region of the blend segments and resulted in better interfacial adhesion. However, when the loading of sericin exceeded 10 wt %, the tensile strength decreased. The poor reinforcing effect of the composite at a higher loading was mainly because the heterogeneous dispersion of aggregated sericin powder in the polymer led to a poor polymer–filler interaction.[30] EB of the composite was found to decrease with the addition of sericin, as shown in Figure 9. This is an expected behavior because the incorporation of sericin particles into the polymer would stiffened the macromolecular chain and, thereby, reduced EB; this is considered an important criteria for higher filler reinforcement.

ac Electrical Conductivity

The variation of the ac conductivity of the sericin-particle-incorporated PVA/PVP blend against the frequency at room temperature is presented in Figure 10. It is clear from the figure that the ac conductivity of the composite was significantly higher than that of the pure blend system. The microparticles in the polymer blends were randomly oriented, and hence, the linkage between the polymer segments through the grain boundary was very poor. This resulted in a lower conductivity.[31] The conductivity of the composite depended on the concentration of filler particles, the filler aggregating tendency, and the shape and morphology of the matrix polymer. We observed from the figure that the conductivity of the composite increased with increasing concentration of sericin particles up to 10 wt %; this was followed by a decrease in the conductivity when the concentration was increased to 15 wt %. The concentration of filler particles after which there is no change in the conductivity, regardless of the further addition of filler, is called the *percolation limit/threshold* of a composite.[32] So when the conductive network is formed at percolation, the matrix changes from an insulating one to a conductive one. At higher concentration of fillers, the individual sericin particles combined to form strong aggregates, and these aggregates were loosely clustered to form higher internal voids, nooks, and crannies in the composite, and this led to the poor

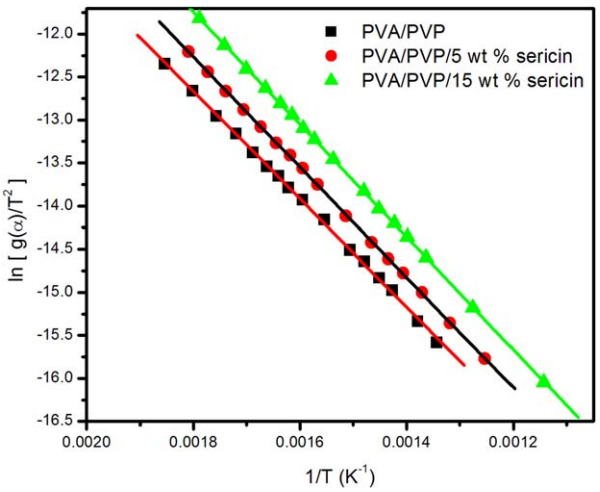

Figure 8. Plot of $\ln[g(\alpha)/T^2]$ versus $1/T$ obtained with the Coats–Redfern method. [Color figure can be viewed in the online issue, which is available at wileyonlinelibrary.com.]

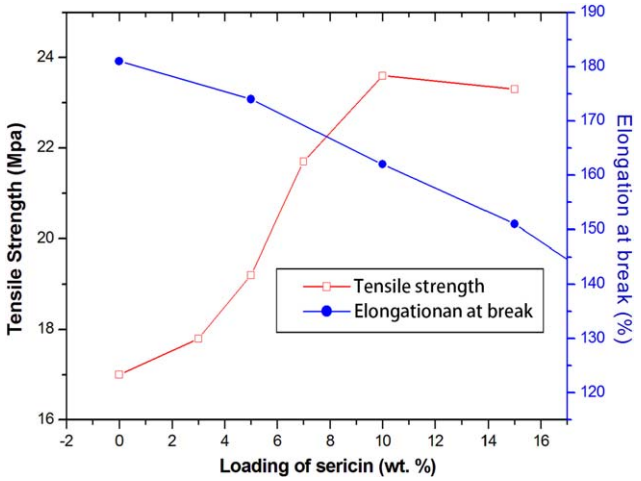

Figure 9. Tensile properties and EB of the PVA/PVP blends with various concentrations of sericin particles. [Color figure can be viewed in the online issue, which is available at wileyonlinelibrary.com.]

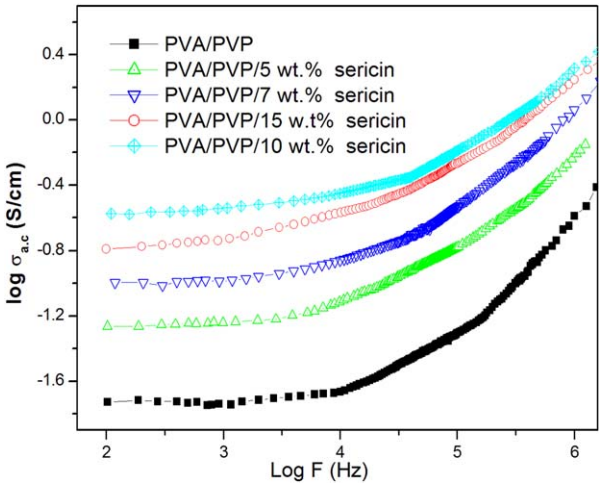

Figure 10. Variation of the ac conductivities of different contents of sericin-filled PVA/PVP blends. σ_{ac} = alternating-current electrical conductivity of sample; F = frequency of AC current. [Color figure can be viewed in the online issue, which is available at wileyonlinelibrary.com.]

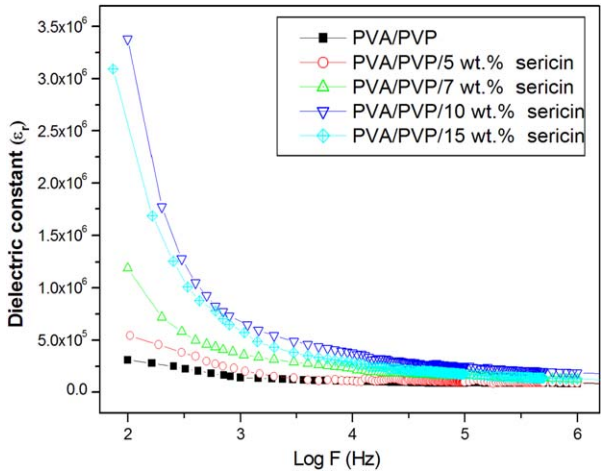

Figure 11. Frequency dependence of the ε_r of the PVA/PVP and PVA/PVP blends with various concentrations of sericin particles. [Color figure can be viewed in the online issue, which is available at wileyonlinelibrary.com.]

electrical conductivity of the resulting polymer matrix, which was confirmed from the SEM analysis.

Dielectric Constant

The dependence of ε_r as a function of the frequency, which ranged from 100 to 10^6 Hz, at room temperature for the PVA/PVP blend and its composites with different concentrations of sericin particle is plotted in Figure 11. We observed from the figure that ε_r of the composite was much higher than that of the pure blend, and the dielectric value increased with increasing concentration of sericin particles. The high dielectric value of the blend composite was mainly due to the increase in the dipole orientation and the interfacial polarization resulting from the presence of polar groups in the sericin particles.[33] An important observation was that the sample with 10 wt % composite exhibited a high ε_r; however, the dielectric value decreased with the further addition of sericin in the PVA/PVP blend. The amide groups present in sericin effectively interacted with the carbonyl or hydroxyl groups of the blends. The polar–polar interaction reduced the cohesive forces operating between the macromolecular chains; this improved the segmental mobility of the polymer matrix. Therefore, more dipoles were developed in the polymer chain through the attachment of sericin particles, which increased ε_r of the composite up to 10 wt % sericin. However, at a higher loading of sericin (15 wt %), the particle-to-particle distance was reduced, and the particles were agglomerated inside the polymer matrix and would not bend to desirable electrical or dielectric properties.[34] We also observed from the figure that ε_r decreased with increasing frequency. The decrease in ε_r with increasing frequency is generally observed in most dielectric materials; this is due to the dielectric relaxation. From the structural point of view, the dielectric relaxation depends on the molecular arrangement of the dielectric material. Therefore, as the frequency increased, the rotational motion of polar dielectric molecules was not sufficiently rapid for the attainment of equilibrium with the field; hence, ε_r was found to decrease with increasing frequency.

tanδ

tanδ is the analysis of the electrical energy associated with the material. The variation of tanδ of the sericin-particle-incorporated PVA/PVP at various frequencies is given in Figure 12. We observed that tanδ decreased steeply as the frequency increased for all of the samples. The tanδ of the composite was significantly higher than that of the pure blend, and also, tanδ increased progressively with increasing concentration of sericin particles up to 10 wt % (the percolation threshold region), whereas tanδ decreased with the further addition of sericin particles. The incorporation of polar fillers led to hydrodynamic and chemical interactions between different functional groups containing sericin and the polar segments of the polymer matrix.[35] The lowest tanδ value of the blend with the 15 wt % sericin/blend composite was due to the hindrance of the orientation of dipoles in the polymer matrix.

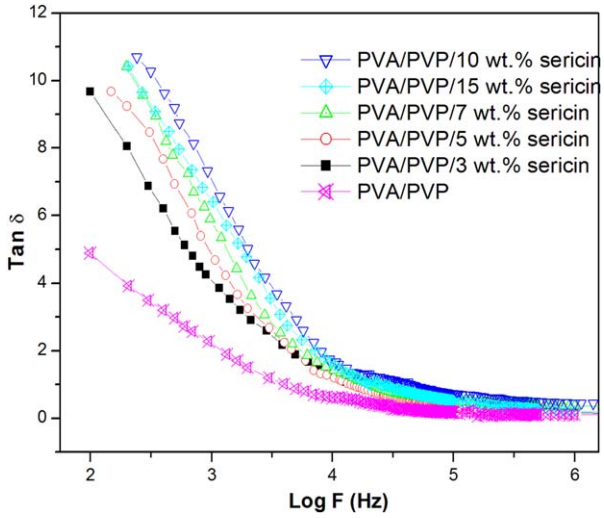

Figure 12. tanδ tangent versus frequency plot for PVA/PVP with sericin powder. [Color figure can be viewed in the online issue, which is available at wileyonlinelibrary.com.]

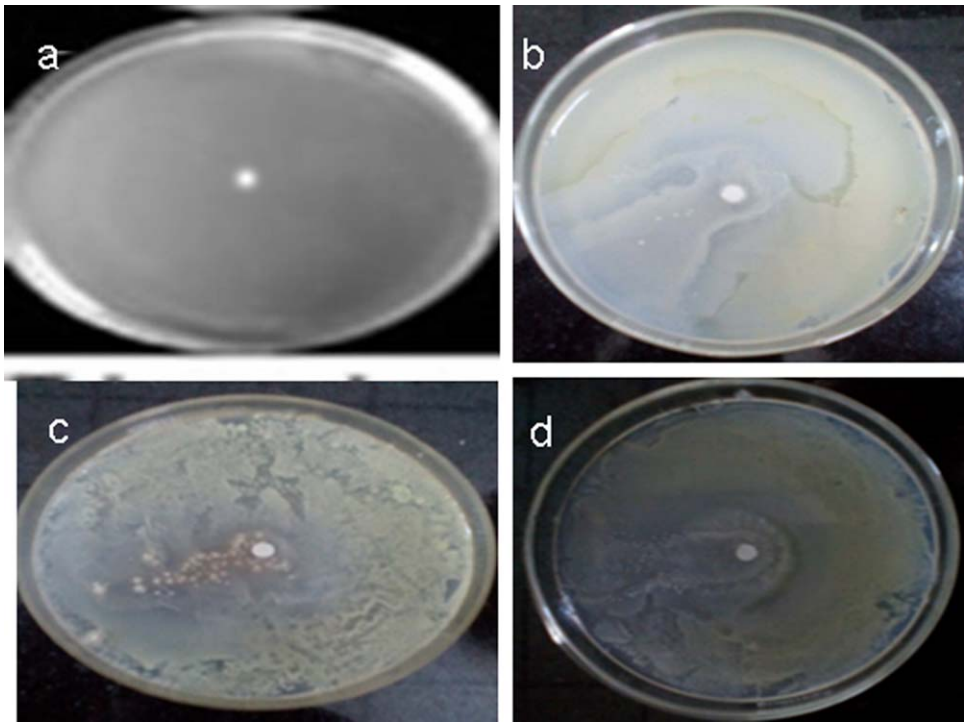

Figure 13. Antibacterial activities of the PVA/PVP blends with different contents of sericin against *S. aureus* bacteria. [Color figure can be viewed in the online issue, which is available at wileyonlinelibrary.com.]

Antibacterial Activity

The photographs given in Figure 13 demonstrate the samples containing the surviving *S. aureus* bacterial colonies in the pure PV/PVP blend and the blend with different dosages of sericin powder. We observed from the figure that the blend did not exhibit a significant inhibitory effect on *S. aureus,* whereas the sericin particles had a significant role in the antibacterial activity of the fabricated composite. The antibacterial properties of the composites were due to the electrostatic interactions between the electronegative microbial surfaces and the positively charged unit of sericin particles.[36] The antibacterial properties of the blended composite increased with increasing dosage of sericin in the polymer blends. This was due to the larger number of electronegative interaction zones present in the sericin particles.

CONCLUSIONS

PVA/PVP blends with different weight percentages of sericin particles were prepared by a simple solution-casting method. The FTIR and UV spectra confirmed the intermolecular interactions of sericin with the blend through the shift in the absorption peaks in the composites. From SEM, it was clear that the addition of sericin to the PVA/PVP affected the morphology of the blend. The XRD study indicated a more ordered structure of blend segments in the polymer composite. The DSC results indicated that T_g and the melting behavior of the PVA/PVP/sericin ternary blend film increased with increasing content of sericin particles. TGA proved that the composites were thermally more stable than the pure blend, and the thermal stability increased with increasing loading of sericin. The retarding process of the composite was due to the intermolecular interactions between the sericin and blend; this impeded heat diffusion into the blend matrix. The value of activation energy for the PVA/PVP/sericin composites increased more than that of the pure PVA/PVP blend; this indicated the higher thermal stability of the composite structure. Therefore, we concluded that sericin particles could be used as a modifier to improve the thermal properties of the PVA/PVP blend. The tensile strength of the composite was higher than that of the pure blend, and the tensile strength increased with increasing concentration of sericin particles, whereas EB decreased with the addition of sericin. Increases in the ac conductivity and dielectric properties, such as ε_r and tanδ, of the composites were observed with increasing loading of sericin up to a certain concentration (10 wt %), and thereafter, the properties decreased. The increase in the electrical properties was due to the interfacial interaction between sericin and the polymer, and the optimum ratio of sericin was found to be 10 wt %. The results from the antibacterial studies revealed that the blend did not show any significant inhibitory effect on *S. aureus* bacteria, whereas the sericin particles played a significant role in the antibacterial activity of the fabricated composite.

ACKNOWLEDGMENTS

The authors thank P. P. Pradyumnan, Department of Physics, University of Calicut, for providing necessary facilities in the department.

REFERENCES

1. Lu, X.; Zhang, H.; Zhang, Y. *J. Polym. Res.* **2014**, *2*, 539.
2. Xu, P.; Yang, F. *Polym. Compos.* **2012**, *33*, 1960.
3. Ramesan, M. T.; Manojkumar, T. K.; Alex, R.; Kuriakose, B. *J. Mater. Sci.* **2002**, *37*, 109.
4. Ramesan, M. T. *Int. J. Polym. Mater.* **2011**, *60*, 1130.
5. Haba, Y.; Narkis, M. *Polym. Eng. Sci. 44*, 1473.
6. Bhajantri, R. F.; Ravindrachary, V.; Poojary, B.; Harisha, A.; Crasta, V. *Polym. Eng. Sci.* **2009**, *49*, 903.
7. Qiao, J.; Fu, J.; Lin, R.; Ma, J.; Liu, J. *Polymer* **2010**, *51*, 4850.
8. Gokmeşe, F.; Uslu, I.; Aytimur, A. *Polym. Plast. Technol. Eng.* **2013**, *52*, 1259.
9. Gupta, D.; Agrawal, A.; Rangi, A. *Indian J. Fibre Text. Res.* **2014**, *39*, 364.
10. Zhang, Y. Q. *Biotechnol. Adv.* **2002**, *20*, 91.
11. Cho, K. Y.; Moon, J. Y.; Lee, Y. W.; Lee, K. G.; Yeo, J. H.; Kweon, H. Y.; Cho, *Int. J. Biol. Macromol.* **2003**, *32*, 36.
12. Padamwar, M. N.; Powar, A. P. *J. Scientific Ind. Res.* **2004**, *63*, 323.
13. Yamada, H.; Nakao, H.; Takasu, Y.; Tsubouchi, K. *Mater. Sci. Eng. C* **2011**, *14*, 41.
14. Aramwit, P.; Sangcakul, A. *Biosci. Biotechnol. Biochem.* **2007**, *71*, 2473.
15. Bhat, P. N.; Nivedita, S.; Roy, S. *Indian J. Fiber Text. Res.* **2011**, *36*,168.
16. Kaitsuka, Y.; Goto, H. *Int. Lett. Chem. Phys. Astronomy* **2015**, *46*, 48.
17. Ramesan, M. T. *J. Elast. Plast.* **2014**, *46*, 303.
18. Sareena, C.; Sreejith, M. P.; Ramesan, M. T.; Purushothaman, E. *Polym. Bull.* **2015**, *72*, 1683.
19. Sareena, C.; Ramesan, M. T.; Purushothaman, E. *Polym. Compos.* **2012**, *33*, 1678.
20. Lee, K. G.; Kweon, H. Y.; Yeo, J. H.; Woo, S. O.; Lee, Y. W.; Cho, C. S.; Kim, K. H.; Park, Y. H. *Int. J. Biomacromol.* **2003**, *33*, 75.
21. Kumar, B. G.; Singh, R. P.; Nakamura, T. *J. Compos. Mater.* **2002**, *36*, 2713.
22. Lakouraj, M. M.; Tajbakhsh, M.; Mokhtary, M. *Iranian Polym. J.* **2005**, *14*, 1022.
23. Ramesan, M. T.; Varghese, M.; Jayakrishnan, P.; Periyat, P. *Adv. Polym. Technol.* DOI: 10.1002/adv21650.
24. Xinqing, C.; Fung, L. A. M. K.; Fong, M. A. K. S.; Kwong, C. W.; Nok, N. G. T.; Lun, Y. K. *Chin. J. Chem. Eng.* **2012**, *20*, 426.
25. Yoshimizu, H.; Asakura, T. *J. Appl. Polym. Sci.* **1990**, *40*, 1745.
26. Aytimur, A.; Kocyigit, S.; Uslu, I. *Polym. Plast. Technol. Eng.* **2013**, *52*, 661.
27. Budrngeac, P. J. *Therm. Anal. Cal.* **2008**, *92*, 291.
28. Ramesan, M. T. *React. Funct. Polym.* **2004**, *59*, 267.
29. Coats, A. W.; Redfern, J. P. *Nature* **1964**, *201*, 68.
30. Ramesan, M. T. *J. Thermoplast. Compos. Mater.* **2015**, *46*, 303.
31. Ramesan, M. T. *Adv. Polym. Technol.* **2013**, *32*, 928.
32. Dahiya, H. S.; Kishore, N.; Mehra, R. M. *J. Appl. Polym. Sci.* **2007**, *106*, 2101.
33. Jayakrishnan, P.; Ramesan, M. T. *AIP Conf. Proc.* **2014**, *1620*, 165.
34. Ramesan, M. T. *Polym. Compos.* **2014**, *35*, 1989.
35. Ramesan, M. T. *J. Appl. Polym. Sci.* **2013**, *128*, 1540.
36. Altan, M.; Yildirim, H. *J. Mater. Sci. Technol.* **2012**, *28*, 686.